

Article

# Spatial Shift of Aridity and Its Impact on Land Use of Syria

Mohammad Rajab Houmsi <sup>1</sup>, Mohammed Sanusi Shiru <sup>1,2</sup>, Mohamed Salem Nashwan <sup>1,3</sup> , Kamal Ahmed <sup>1</sup>, Ghaith Falah Ziarh <sup>1</sup> , Shamsuddin Shahid <sup>1</sup> , Eun-Sung Chung <sup>4</sup>  and Sungkon Kim <sup>4,\*</sup>

<sup>1</sup> School of Civil Engineering, Faculty of Engineering, Universiti Teknologi Malaysia (UTM), Johor Bahru 81310, Malaysia; eng.rajabhoms@gmail.com (M.R.H.); shiru.sanusi@gmail.com (M.S.S.); m.salem@aast.edu (M.S.N.); kamal\_brc@hotmail.com (K.A.); eng.ghaith.ziarh@gmail.com (G.F.Z.); sshahid@utm.my (S.S.)

<sup>2</sup> Department of Environmental Sciences, Faculty of Science, Federal University Dutse, Dutse P.M.B. 7156, Nigeria

<sup>3</sup> Construction and Building Engineering Department, College of Engineering and Technology, Arab Academy for Science, Technology and Maritime Transport (AASTMT), Cairo 2033, Elhorria, Egypt

<sup>4</sup> Faculty of Protection and Safety Engineering, Seoul National University of Science and Technology, 232 Gongneung-ro, Nowon-gu, Seoul 01811, Korea; eschung@seoultech.ac.kr

\* Correspondence: skkim@seoultech.ac.kr; Tel.: +82-2-970-6571

Received: 13 October 2019; Accepted: 22 November 2019; Published: 10 December 2019



**Abstract:** Expansion of arid lands due to climate change, particularly in water stressed regions of the world can have severe implications on the economy and people's livelihoods. The spatiotemporal trends in aridity, the shift of land from lower to higher arid classes and the effect of this shift on different land uses in Syria have been evaluated in this study for the period 1951–2010 using high-resolution monthly climate data of the Terrestrial Hydrology Research Group of Princeton University. The trends in rainfall, temperature and potential evapotranspiration were also evaluated to understand the causes of aridity shifts. The results revealed an expansion of aridity in Syria during 1951–1980 compared to 1981–2010. About 6.21% of semi-arid land was observed to shift to arid class and 5.91% dry-subhumid land to semi-arid land between the two periods. Analysis of results revealed that the decrease in rainfall is the major cause of increasing aridity in Syria. About 28.3% of agriculture land located in the north and the northwest was found to shift from humid to dry-subhumid or dry-subhumid to semi-arid. Analysis of results revealed that the shifting of drylands mostly occurred in the northern agricultural areas of Syria. The land productivity and irrigation needs can be severely affected by increasing aridity which may affect food security and the economy of the country.

**Keywords:** aridity; shift of arid lands; Mann–Kendall test; land use; Syria

## 1. Introduction

The transition of aridity is considered as a foremost and assertive impact of global climate change. Evapotranspiration is supposed to increase due to a rise in temperature, which along with the changes in precipitation patterns could alter atmospheric water balance and aridity [1–8]. Increasing aridity with the changes in climate has been noticed in different regions of the Earth [9–12]. An increase in arid lands by 3.1% between 1980–2010 and 1951–1980 has been reported by Liu, Sun [13]. Studies also reported a continuous increase in aridity in the context of climate change. Koutroulis [14] projected a 7% increase in global drylands in the last part of the present century while Feng and Fu [15] projected an increase of 10%. The increase in aridity would compel more than 24% population to live under water stress by the end of this century [16].

Though an increasing trend in global aridity has been reported, the increase would not be homogeneous in all regions. In many regions, it will be insignificant due to the increase in rainfall. Ahmed, Shahid [17] also reported a decrease in aridity in some parts of Pakistan. Studying the changes in aridity at the regional scale is very important to understand the magnitude and spatial pattern of the changes as well as the shift of lands from one class of aridity to another arid class. Such information is particularly important for agriculture-based countries where the shifting of dryland can have a considerable implication in the economy and people's subsistence.

The temperature in the drylands of western Asia is increasing at a higher rate compared to other regions [18–20]. The high increase in temperature caused a rise in potential evapotranspiration (PET) by a few folds in the region [21]. A concurrent decrease in precipitation is also noticed in some of the regions [22,23]. The rapid increase in PET and decrease in precipitation are supposed to increase the aridity in the region. However, studies related to changes in aridity are still very limited in the region. Few studies on aridity trends have been conducted in some regions like Iran [24–26], Iraq [27], Turkey [28], Lebanon [29,30] and Egypt [31]. But such studies are still lacking in the majority of the regions, particularly for conflict-affected countries.

Syria, located in East Asia, is a country highly vulnerable to climate change. Long-time wars and conflicts have made the country more susceptible to any impact due to climate change. A large change in the climate of recent years and its impacts on the agriculture of the country has been reported [32,33]. Agriculture contributes between 26–36% of the total national gross domestic product of Syria [34]. The majority of the people of the country depend on agriculture for their livelihood. The expansion of arid lands would be devastating for the socio-economy of the country [35] particularly with an expected increase in future temperatures and more erratic rainfalls in many parts of the globe including Syria [11,36–40].

Spatiotemporal changes in aridity and the shifting of arid lands between different arid classes have been assessed in the present study. The gridded monthly data of precipitation, temperature, humidity and wind speed data of the Terrestrial Hydrology Research Group of Princeton University having a spatial resolution of  $0.25^\circ$  were used to estimate the aridity changes for the period 1951–2010. The modified version of the Mann–Kendall test which can remove the effect of natural variability from unidirectional trend was used to evaluate the impact of global warming driven climate change on aridity. Additionally, the spatial changes in aridity for two periods, 1951–1980 and 1981–2010 were estimated. A number of studies revealed that the aridity trend was more pronounced after the 1980s [41,42]. Therefore, this study was conducted to assess how aridity in Syria has changed since 1980. Aridity makes an ecosystem fragile and thus more prone to natural disasters. It reduces land productivity and contributes to losses in biodiversity. The findings of this study could help in the long-term management of land and natural resources and policy formulation for the mitigation of climate change impacts on agriculture, ecology and natural hazards in Syria.

## 2. Study Area and Datasets

Syria, with a latitude of  $32^\circ$ – $38^\circ$ , and longitude of  $35^\circ$ – $43^\circ$ , is located in the north of the Arabian Peninsula (Figure 1). Its topography consists of mountain ranges in the west and steep lands in the east. Although the area of Syria is relatively small (185,180 km<sup>2</sup>), it has diversity in climate. According to the Koeppen–Geiger classification, the climate of Syria has a mild Mediterranean climate in the west, semi-arid in the middle and a hot desert climate in the east.

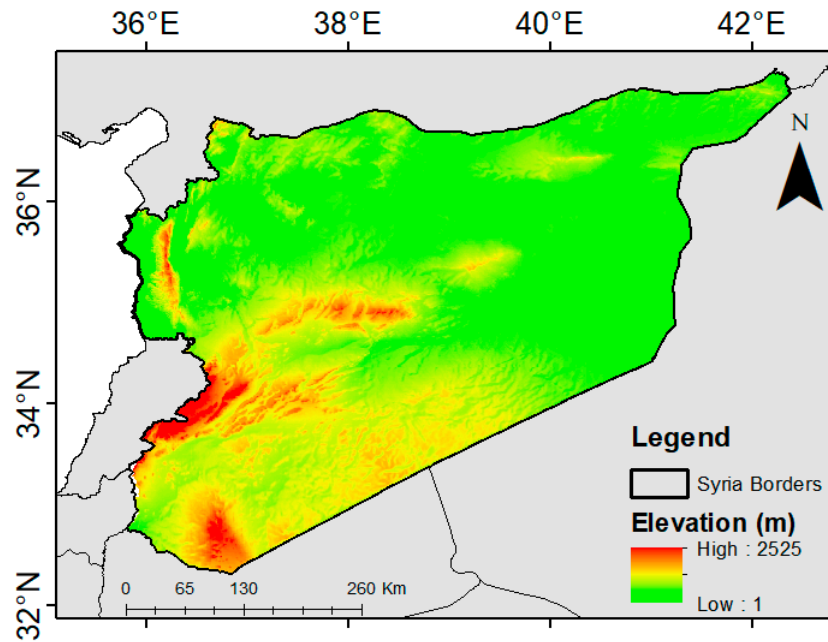


Figure 1. The location of Syria and its topography.

Syria has two major seasons: hot and dry summer (May to October) and cool and wet winter (November to April). The precipitation occurs in Syria mainly in winter (November to May) by moist air carried out by the Mediterranean wind. The rainfall in the country ranges between 75 mm to 1000 mm per year. Spatial distributions of annual mean rainfall and the annual average of daily temperature of Syria are shown in Figure 2. Most rain in the country occurs in the Mediterranean coastal regions and very less in the inland. The mean temperature of the country ranges from 23 °C in the eastern coast to 12 °C in the western desert. January is the coldest month (annual mean temperature of 7 °C) and August is the hottest (27 °C). Recently, Syria faced several long-term severe droughts [43], which caused crop failure, large migration and economic damages prior to the civil war unrest [44]. Nevertheless, droughts impacts became more severe with the current unrest in Syria [45]. The droughts were caused by a decrease in rainfall amounts and an increase in evapotranspiration [46]. Romanou, Tselioudis [47] remarked a significant rise of evaporation in the west of the country during 1988–2006.

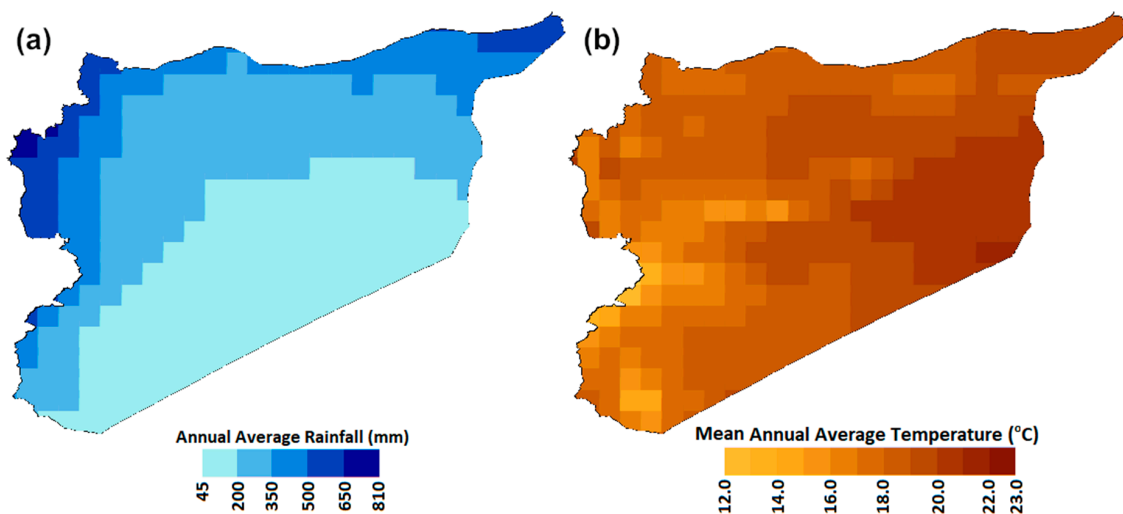


Figure 2. The spatial variability in annual average of (a) total rainfall, (b) daily mean temperature over Syria estimated by Global Meteorological Forcing Dataset for Land Surface Modeling (PGF) datasets for the period 1951–2010.

In this study, the Global Meteorological Forcing Dataset for Land Surface Modeling (PGF) dataset developed by the Land Surface Hydrology Research Group of Princeton University [48] was used. It was developed by integrating several datasets including the reanalysis datasets of the National Centers for Environmental Prediction (NCEP) and National Center for Atmospheric Research (NCAR), Global Precipitation Climatology Project (GPCP), the Tropical Rainfall Measuring Mission (TRMM) and the World Meteorological Organization (WMO) Solid Precipitation Measurement Intercomparison [48]. The PGF dataset was used in this study due to long-term availability of complete records. Estimation of PET using the Penman–Monteith method needs a number of meteorological variables. For this purpose, PGF daily near-surface meteorological variables including maximum and minimum temperatures, relative humidity, and wind speed at a 0.25° spatial grid were used in this study. Solar radiation was estimated using the solar radiation model proposed by [49]. PGF data has been widely used for several hydroclimatic studies in the Middle East [19,50,51] and Asia [4,52,53]. The information about different datasets, their providers, period of availability, period of data used in this study, and the spatial resolution are given in Table 1.

**Table 1.** Information on climate datasets used in the present study.

Dataset	Institute	Data Availability Period	Data Period Used	Spatial Resolution
Rainfall				
Max Temperature	Land Surface			
Min Temperature	Hydrology Research	1948–2010	1951–2010	0.25 × 0.25
Solar Radiation	Group of			
Relative Humidity	Princeton University			
Vapor Pressure				

### 3. Methodology

#### 3.1. Aridity Index

Aridity Index (AI) is a widely used measure to describe the water-deficient of a given climate. The widely used AI [54] characterizes aridity by the proportion of precipitation ( $P$ ) to the potential evapotranspiration (PET) as shown in Equation (1);

$$AI = \frac{P}{PET} \quad (1)$$

where both  $P$  and  $PET$  are the average annual values and expressed in the unit of length. Table 2 presents the five classes of the degree of aridity based on the AI value. The intensity of aridity increases by the decrease of AI value.

**Table 2.** Aridity classes based on aridity index (AI) values.

AI Range	Aridity Class
$AI < 0.03$	Hyper-arid
$0.03 \leq AI < 0.20$	Arid
$0.20 \leq AI < 0.50$	Semi-arid
$0.50 \leq AI < 0.65$	Dry-subhumid
$AI \geq 0.65$	Humid

#### 3.2. Calculation of Potential Evapotranspiration

The AI value significantly depends on the method used for the estimation of PET. Several methods are available for estimating PET. They vary in the degree of accuracy depending on the availability of data, temporal scale, application and climate type [55,56]. Studies revealed that the Food and Agriculture Organization (FAO) Penman–Monteith model [57] can measure PET most accurately in any regions of the globe [54]. Therefore, it has been used as a customary method for PET estimation

in all over the world [58]. In this study, the FAO Penman–Monteith empirical method of estimating potential evapotranspiration was used as follows:

$$PET = \frac{\Delta R_n + 0.4244 (1 + 0.536u_2)(e_s - e_a)}{(\Delta + 0.067)(2.501 - 0.00236T)} \quad (2)$$

where PET is in mm/day,  $u_2$  is the wind speed at 2 m above the surface (m/h),  $T$  is the temperature ( $^{\circ}\text{C}$ ),  $e_s$  is the saturation vapor pressure (KPa),  $e_a$  is the actual vapor pressure (KPa),  $\Delta$  is the gradient of the saturation pressure curve (KPa/ $^{\circ}\text{C}$ ), and  $R_n$  is the net radiation of the earth's surface (MJ/m<sup>2</sup>/day).

The mean saturation vapor pressure ( $e_s$ ) was calculated from air temperature while the actual vapor pressure ( $e_a$ ) was calculated from relative humidity. The slope of saturation vapor pressure was calculated from saturation vapor pressure and temperature. Details of the calculation are given in [57].

### 3.3. Sen's Slope

Sen's slope is a non-parametric estimator of the rate of change over a period of time [59]. It is estimated as the median of the rate of change between two consecutive data points ( $Q$ ) and estimated as:

$$Q = \frac{x_i - x_k}{i - k} \text{ for } N = 1, 2, 3, \dots, n \quad (3)$$

where  $x_i$  and  $x_j$  are two data points at time  $i$  and  $k$ .

### 3.4. Modified Mann–Kendall Test

The Modified Mann–Kendall (MMK) test is a robust test against the effect of long-term persistence (LTP) in data. It was proposed by Hamed [60] and was widely used ever since [4,5,11,18,19,23,51,61–65]. The MMK test calculates the equivalent normal variates of the rank ( $R_i$ ) of a de-trended series of length,  $n$  as:

$$Z_i = \phi^{-1} \left( \frac{R_i}{n + 1} \right) \text{ for } i = 1 : n \quad (4)$$

where  $\phi^{-1}$  is the inverse standard normal distribution function. The scaling coefficient or Hurst coefficient,  $H$  can be calculated by maximizing the log-likelihood function [66];

$$\log L(H) = -\frac{1}{2} \log |C_n(H)| - \frac{Z^T [C_n(H)]^{-1} Z}{2\gamma_o} \quad (5)$$

where  $|C_n(H)|$  is the determinant of the correlation matrix of lag for a given  $H$ ;  $Z^T$  is the transposed vector of equivalent normal variates  $Z$ ; and  $\gamma_o$  is the variance of  $z_i$ . Significance of  $H$  is determined from the mean ( $\mu_H$ ) and the standard deviation ( $\sigma_H$ ) for  $H = 0.5$  [60];

$$\mu_H = 0.5 - 2.87n^{-0.9067} \quad (6)$$

$$\sigma_n = 0.7765n^{-0.5} - 0.0062 \quad (7)$$

If  $H$  is found to be significant at the 0.05 significance level, the variance of  $S$  for given  $H$  is calculated as;

$$V(S)^{H'} = \sum_{i < j} \cdot \sum_{k < l} \frac{2}{\pi} \sin^{-1} \left( \frac{\rho |j - i| - \rho |i - l| - \rho |j - k| + \rho |i - k|}{\sqrt{(2 - 2\rho |i - j|)(2 - 2\rho |k - l|)}} \right) \quad (8)$$

where  $\rho_1$  is the auto-correlation function for given  $H$  and  $V(S)^{H'}$  is the biased estimate. The unbiased estimate  $V(S)^H$  is calculated as below:

$$V(S)^H = V(S)^{H'} \times B \quad (9)$$

where  $B$  is a function of  $H$ . The significance of trend is then estimated using  $Z$  statistics;

$$z = \begin{cases} \frac{S-1}{\sqrt{V(S)^H}} & \text{if } S > 0 \\ 0 & \text{if } S = 0 \\ \frac{S-1}{\sqrt{V(S)^H}} & \text{if } S < 0 \end{cases} \quad (10)$$

The null hypothesis of no trend is rejected at the 0.05 significance level when  $|Z| > 1.96$ . Further details of the MMK test can be found in [60].

## 4. Results

### 4.1. Estimation of Spatial Distribution of Potential Evapotranspiration

The maps of the meteorological variables employed for the PET calculation using the Penman—Monteith method are presented in Figure 3. Annual means of daily relative humidity and wind speed in Syria were found to vary from the coast in the west to the inland. The gradient of relative humidity was found to decrease from 75% in the northwest humid region to 45% in the desert located in the southeast. The wind speed was found to decrease from 4.3 m/h in the northwest to less than 2.8 m/h in the northeast. Solar radiation was found to vary according to latitude. The highest amount of solar radiation ( $7.3 \text{ W/m}^2$ ) was estimated in the southeast of the country.

Anomaly in different meteorological variables and aridity over the study period (1951–2010) is shown in Figure 4. The areal average values of meteorological variables over the period 1951–2010 were deducted from the mean for the period to prepare the anomaly series. The anomaly series provided a visual presentation of the changes in aridity and different meteorological variables over time. The figure shows almost no change in maximum temperature while an increase in minimum temperature in recent years. The PET was observed to increase while the rainfall decreased in recent years. Almost no change in areal average relative humidity was noticed. The AI in Syria was found to decrease due to an increase in PET and a decrease in rainfall.

The PET estimated using the meteorological variables is shown in Figure 5. The PET was found to increase from 1600 mm in the northwest to 2800 mm in the southeast. The high PET compared to rainfall has resulted in the climate of most parts of Syria to be arid.

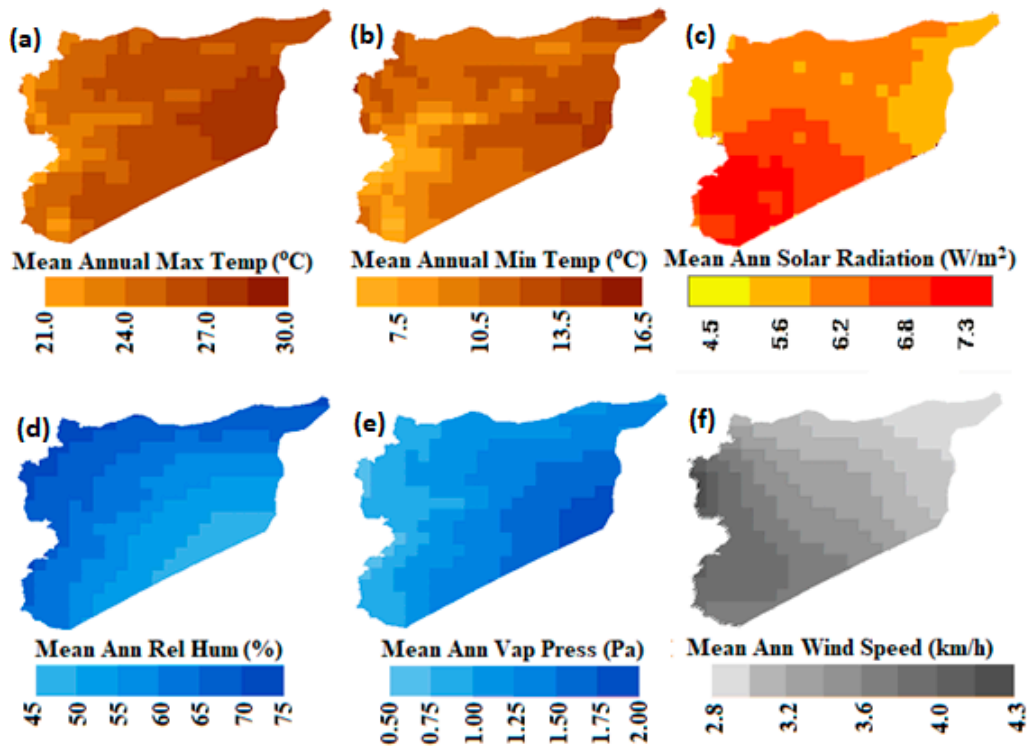


**Figure 3.** Geographical distribution of annual mean of daily (a) maximum temperature (°C); (b) minimum temperature (°C); (c) solar radiation (W/m<sup>2</sup>); (d) relative humidity (%); (e) vapor pressure (kPa) and (f) wind speed (m/h).

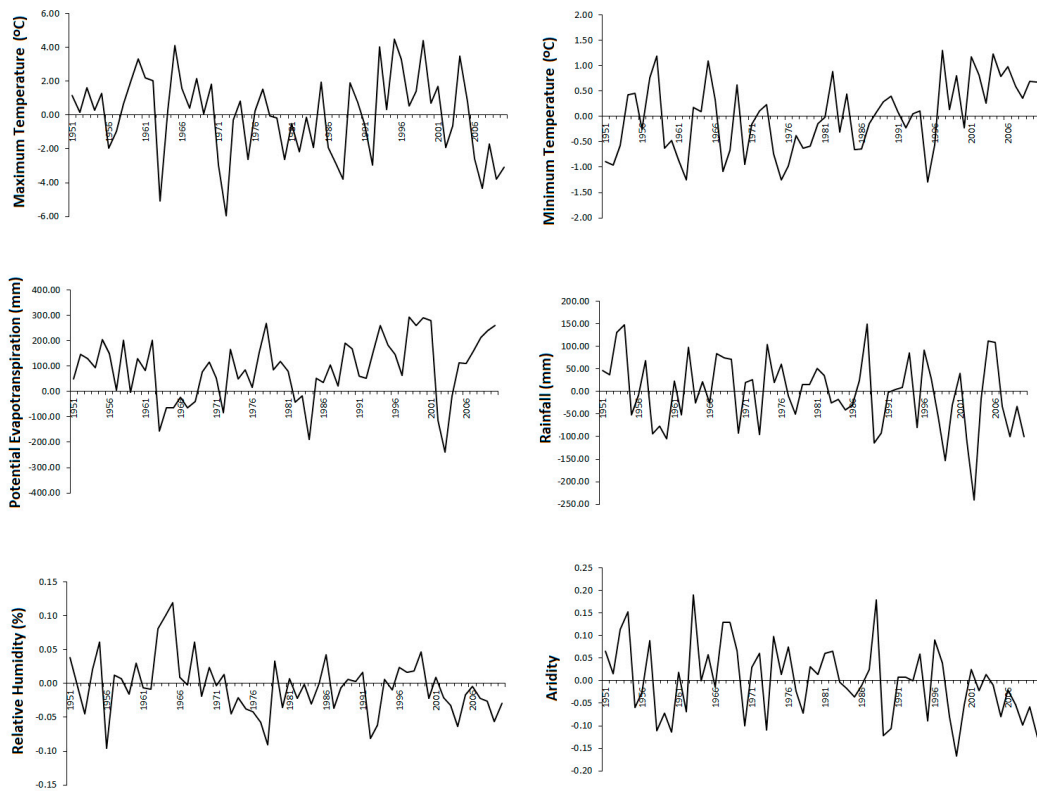


**Figure 4.** Anomaly in aridity and different meteorological variables over the study period (1951–2010).

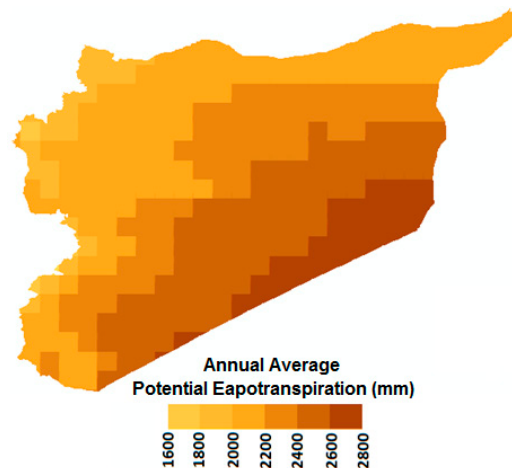


**Figure 5.** Spatial distribution of potential evapotranspiration (mm) estimated using the Penman–Monteith method.

#### 4.2. Spatial Patterns of Annual Aridity and Trends

The spatial pattern of AI estimated for the period 1951–2010 is given in Figure 6a. The figure revealed that Syria has a large area with an arid climate. The climate in about 44% of the land in the southeast is arid. The area is mostly covered by desert with very little potential for any kind of agriculture or farming activities. About 40% of the land in the north and the west are semi-arid. The rest of the land in the northeast and northwest are dry-subhumid (7%) and humid (9%). Land in dry-subhumid to humid regions is widely used for agriculture. Besides, a substantial amount of land in the north located in the semi-arid climate is also used for agriculture and farming. Overall, the climate of the country can be classified as arid.

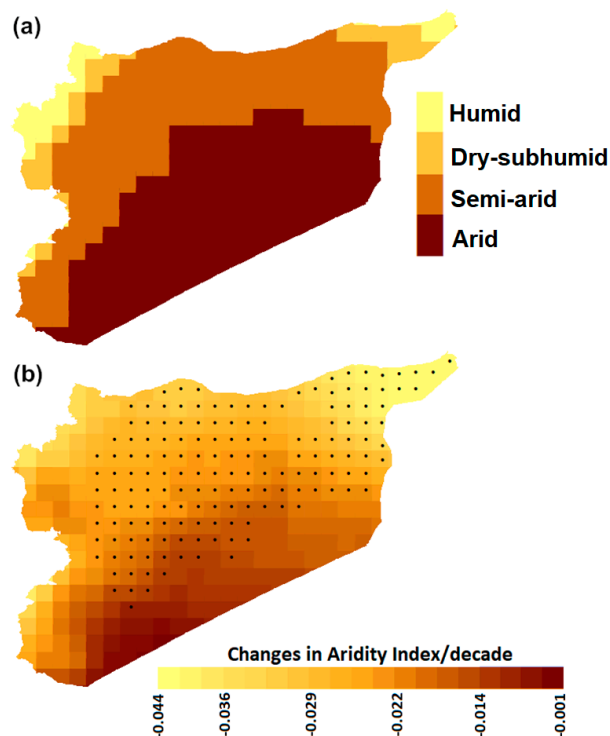


**Figure 6.** (a) Spatial distribution of aridity; (b) trends in aridity index estimated for the period 1951–2010. The color ramp in trend figure shows the rate of change and the dots represent the significance of the change.

The trends in AI values for the period 1951–2010 was estimated using MMK test and presented in Figure 6b. The results of the trends in the figure revealed the significant increase in aridity (decrease in AI) over a large area of the country. Increases are mostly found in the semi-arid region in the north and dry-subhumid and humid regions in the northeast. The aridity in most of the arid regions in the southeast was not found to be changed. Aridity in the eastern coastal region was also not found to significantly be changed. Overall, the results revealed a gradual drying of climate for Syria.

#### 4.3. The Shift in Aridity

The spatial pattern of the shift of land from one arid class to another was investigated by mapping the differences between the aridity observed in 1951–1980 and 1981–2010. The aridity maps for those periods and the map showing the shift of aridity are shown in Figure 7. It was noticed that aridity for both periods had more or less same patterns. However, the difference showed in Figure 7c revealed that a large area has changed from semi-arid to arid in the northeast. A large part of the arid region in the center of the country has also become hyper-arid. It can be also noted that a small area in the southern region also turned arid. A shift from humid to dry-subhumid and dry-subhumid to semi-arid in the northeast corner and western side was also witnessed.

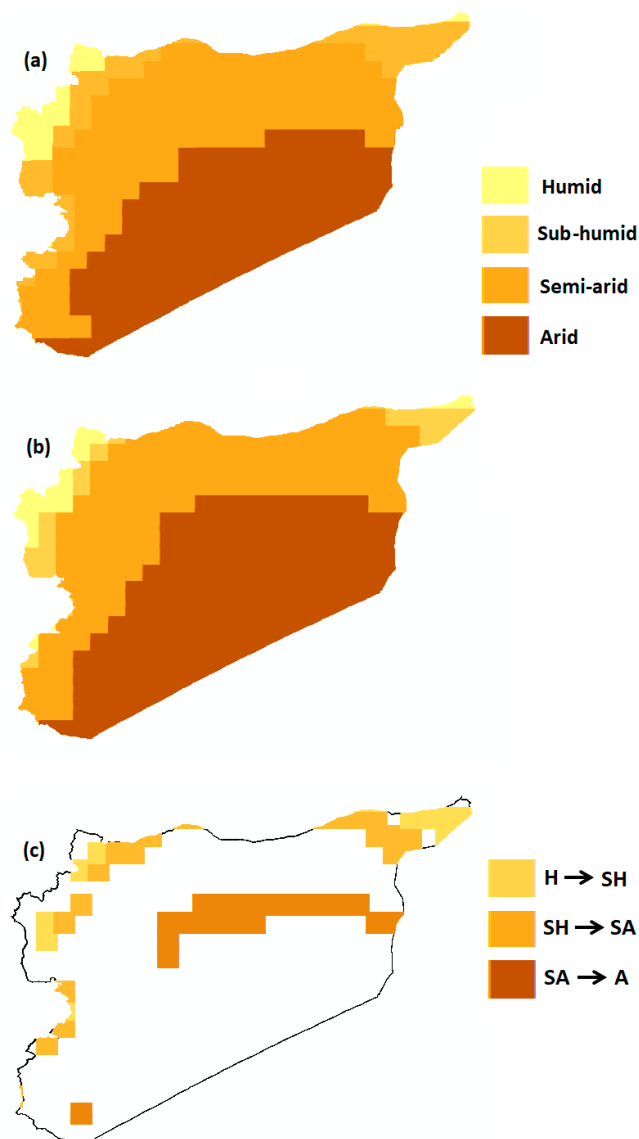


**Figure 7.** Changes in the spatial patterns of aridity (a) 1951–1980; (b) 1981–2010, and (c) difference in aridity between (1951–1980) and (1981–2010).

The percentage of the area shifted from one to another arid class between 1951–1980 and 1981–2010 are given in Table 3. It was observed that 3.55% of the humid area turned into dry-subhumid. Similarly, 5.91% of the area was shifted from dry-sub humid to semi-arid and around 6.21% of the area was changed from the semi-arid to the arid climate. About 40.8% of the land was arid during 1951–1980 which was increased to about 47% during 1981–2010. The results indicate that Syria has turned dryer in recent years, compared with the early period (1951 to 1980).

**Table 3.** The land (%) shifted from one to another aridity class between the periods, 1951 to 1980 and 1981 to 2010.

Aridity Class	1951–1980	1981–2010	Percentage Change	Change to
Humid	10.08	6.50	3.55	Sub-humid
Dry-subhumid	8.87	6.50	5.91	Semi-arid
Semi-arid	40.23	39.96	6.21	Arid
Arid	40.82	47.04	–	–

#### 4.4. Geographical Distribution of the Trends in Rainfall, Temperature and Potential Evapotranspiration

In order to understand the causes of aridity shifts, the geographical distribution of the trends in rainfall, temperature, and PET are given in Figure 7. Changes in rainfall, temperature, and PET were estimated using Sen's slope and significance of changes were verified using a modified version of the MMK test at 0.05 significance level for the period 1951 to 2010. The changes in rainfall were estimated between 4 to  $-32.0$  mm/decade. The significant reduction in precipitation was noticed in the north and northeast. The decreasing rate was found more than 32 mm/decade in the northeast where annual total rainfall is about 800 mm. The rainfall decreased in the northern semi-arid region by 12 to 16 mm/decade where the annual average precipitation is between 300 and 400 mm. This indicates that precipitation in the north and northeast of the country is decreasing rapidly.

The temperature of the country was found to significantly increase at all locations. The increase was found high in the high-temperature region and relatively less where the temperature is comparatively lower. The highest increases are observed in the east, particularly in the northeast ( $0.28$  °C/decade). Besides, it was found to rapidly increase in the northwest ( $0.17$  °C/decade). In contrast, PET was not observed to significantly increase at any location except at a single point situated in the western desert. The spatial pattern of PET trend was found to follow the temperature trend, which indicates that temperature has a role in shaping the PET of the country. The rising temperature was the cause of PET increase in most parts of the country, but the increases are not statistically significant yet. But the rising trend of temperature can cause an increase in PET in the future.

The aridity trend map and the aridity shift map in Figures 6 and 7 respectively were analyzed with the trend maps of Figure 8 to evaluate the effect of rainfall and temperature on aridity in Syria. It was found that the AI reduced significantly (or aridity increased significantly) in the region where rainfall decreased more, such as the north and northeast of the country. Aridity in the northwest of the country increased though rainfall has not been changed in the region. This may result in a rise in temperature. Overall, the results showed that the increasing aridity in the semi-arid region was mostly due to the decrease in rainfall, while the increasing aridity in the humid and dry-subhumid region of the northwest resulted from the increase in temperature.

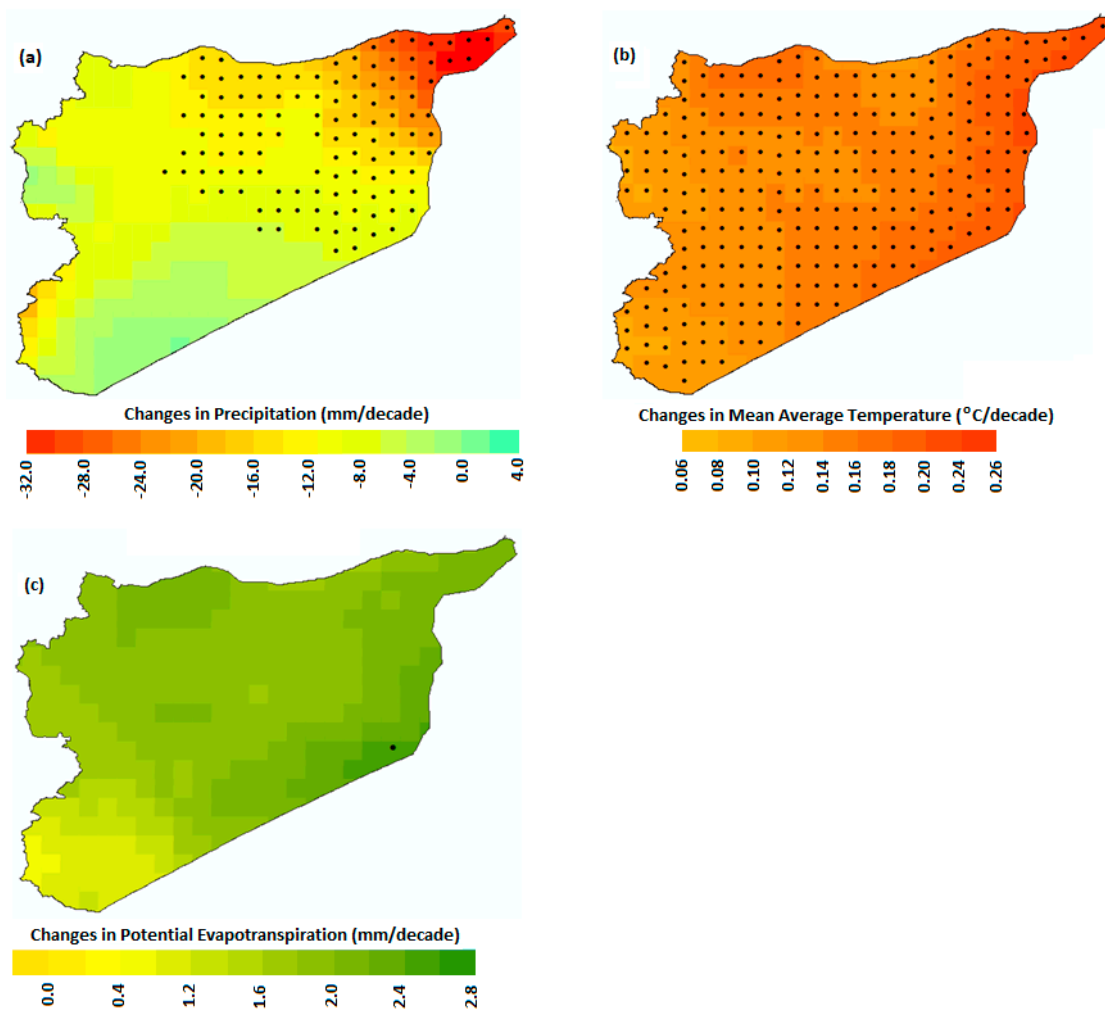


**Figure 8.** Geographical distribution of the trends in (a) rainfall, (b) temperature and (c) potential evapotranspiration from 1951 to 2010. The significant trends at 0.05 level estimated by the Mann–Kendall trend test are presented using dots.

#### 4.5. Impact of Aridity Shift on Land Use

The land use map of Syria is presented in Figure 9. About 65% of land in the south and southwest is categorized as a desert or steep lands and pasture with very little grazing capacity. The climate in these two regions is arid or near to hyper-arid. About 33% of the land, located in the north and the west are cultivable, among which 91.7% is used for cultivation. This indicates intense agricultural activities in the cultivable lands in the north and west of Syria. The climate of the region is mostly semi-arid to humid. The rest of the land (3%) is forested land, which is sparsely distributed over the country, but most are placed in semi-arid region. The crops lands in the north are mostly irrigated. Besides, there is rainfed agriculture in some regions of the northeast and west, particularly, in the northwest.

It was difficult to quantify the impact of aridity shifting on different land uses accurately due to the coarse resolution of gridded data. However, the aridity shifts map shown in Figure 7c was overlaid on the land use map of Figure 9 to quantify the impact of dryland shift on land use and agriculture of Syria. The percentage of different land use affected by aridity shift is given in Table 4. In term of the affected area, the agriculture land in the northeast and west, particularly in the northwest was most affected by aridity shift. About 28.3% of agriculture land has been shifted from humid to dry-subhumid or dry-subhumid to semi-arid. In term of percentage of the affected area, forested land will be affected most. About 32.7% of forested land has been shifted to lower arid class to higher arid class. Besides,

13.1% of the land in the middle of the country with scattered agriculture has experienced a shift from semi-arid to arid land.

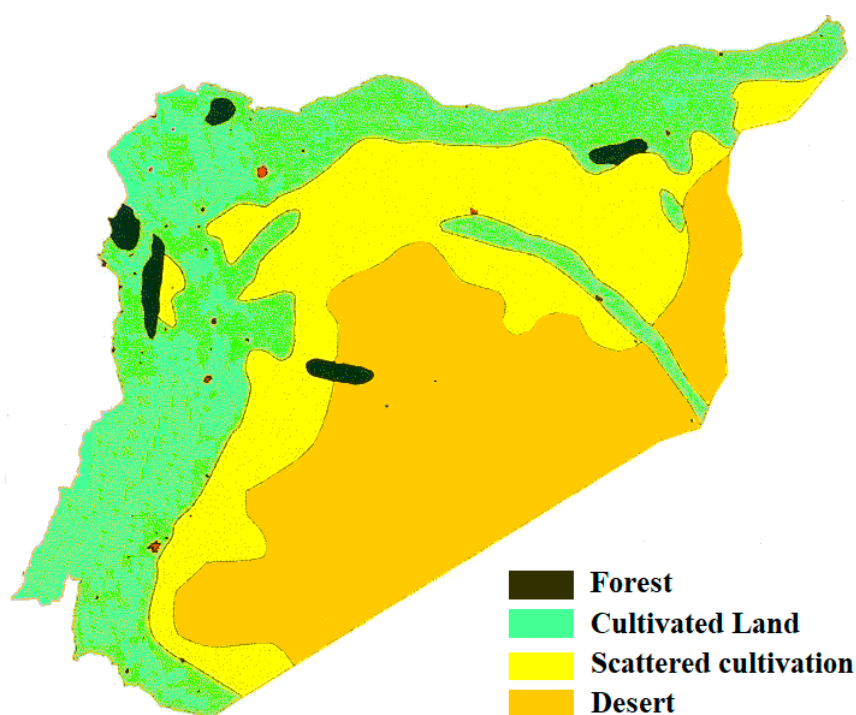


Figure 9. The land use map of Syria.

Table 4. Land use in Syria affected by aridity shift between 1951–1980 and 1981–2010.

Land Use	Aridity Shift	Aridity Shifted To
Forest	32.7%	Semi-arid and subhumid
Cultivated land	28.3%	Semi-arid and subhumid
Scattered cultivation	13.1%	Arid

## 5. Discussion

Spatiotemporal trends in aridity, the shift in arid land from one class to another, and the impact of aridity shift on different land uses of Syria were assessed in this study using high resolution gridded climate data. The results revealed a decrease in aridity or an increase in aridity in Syria over the period 1951–2010. Increase and decrease in aridity has been noticed in different parts of the globe. Among those a number of studies reported dry regions to become drier more extensively compared to drying of wet regions [67,68]. The same has been observed in Syria, where dry-subhumid and semi-arid regions are found to be shifted to semi-arid and arid, respectively. The time series analysis of areal average aridity and different climatic variables showed an increasing tendency in PET with a decrease in rainfall in recent years. An increase in PET and a decrease in rainfall caused a decrease in AI or more aridity in Syria. The analysis of time series data revealed the decrease in AI become visible in recent years (after the 1990s). This is mainly due to a decrease in rainfall in Syria in recent years. Pour et al. [2] examined the cause of aridity shifts in different climate zones of Iran, bordering Syria. The study showed that a gradual reduction of rainfall is the primary driver of increasing aridity in the arid and semi-arid regions.

This is the first attempt to assess the trends in aridity and shift of arid lands in Syria. Therefore, it was feasible to validate the results of the study with earlier findings. However, the results of this study correspond to the aridity trends in a nearby country. An increasing trend in aridity at 45% of

the observed locations of Iran, bordering Syria was estimated by Shifteh Some'e, Ezani [69] during 1966–2005. Tabari, Hosseinzadeh Talaei [26] also reported a rising trend in aridity in most parts of Iran during 1966–2005. Pour, Abd Wahab [2] reported a significant shift of 4.84% semi-arid land to arid land in Iran between 1951–1980 and 1987–2016. Deniz, Toros [70] reported a shift of semi-arid region to higher aridity in Turkey during 1991–2006 compared to 1960–1990. Şarлак and Agha [27] reported increasing aridity in recent years in the predominantly arid country of Iraq. In recent years an increasing tendency in aridity is also reported in Iraq [27].

The anomaly time series of areal average maximum and minimum temperature of Syria revealed almost no change in maximum temperature while an increase in minimum temperature. This indicates a decrease in the diurnal temperature range (DTR) in Syria in recent years. The decrease in DTR is considered as an indication of anthropogenic climate change [18,51,71–73]. Therefore, it can be remarked that the recent changes in aridity in Syria may be due to global warming-induced climate change.

An increase in rainfall with the rise in temperature due to global warming has been noticed in many regions of the globe [5,74–76]. In contrast to many other areas, the precipitation in some areas of Syria was observed as decreasing. Pour et al. [2] reported that the process of atmospheric saturation under a warmer climate takes more time which eventually delays the onset of precipitation. A higher amount of water vapor will be transported to higher latitudes under a warmer climate by the atmospheric circulation before precipitation can be formed. This has been particularly noticed in arid and semi-arid regions of the Middle East [77]. Therefore, rises in temperature in the region caused a decrease in precipitation. It can be anticipated from the results that a continuous rise in temperature in the region due to global warming may cause a further decrease in precipitation and more aridity in the region in future.

The overlapping of land use map on the land shift map revealed a shift of different drylands to higher arid classes mostly in the irrigated agricultural lands in the north and the northwest of Syria. The aridity reduces soil micronutrient and thus, land productivity [78]. It also increases land erosion, sedimentation and dust particulates in the air which eventually reduces the suitability of land of agriculture and grazing. Reduction of biodiversity, damage to ecology and deterioration of the environment is commonly noticed with the increase of aridity. This indicates a shifting of aridity which can have severe implications for agriculture and the environment of the country.

The increase of aridity always causes an increase in irrigation needs, and thus, water stress. Chowdhury, Al-Zahrani [79] found that an increase of temperature by 1 °C causes an increase in irrigation demand by 2.9% in the region. Ragab and Prudhomme [80] found that decreasing rainfall has caused a large increase in irrigation needs in the arid region of the Middle East. As a country with limited water resources, the increase in irrigation needs would certainly cause agricultural water stress in the country. A further rise in temperatures with global warming may drive a further increase in irrigation demand and more water stress. The impact would be more devastating due to the growing aridity in agriculture regions in the north and the northwest. Increasing demand for irrigation and possible increase of water stress under climate change scenarios have reported in neighboring countries of Syria. Azad, Behmanesh [81] reported increasing water stress for the winter wheat crop in northern Iran. Onder, Akiskan [82] reported higher irrigation needs and crop water stress in southern Turkey.

An increase in aridity may make the country more susceptible to natural disasters, particularly droughts which are the major cause of crop failure in Syria. Prolonged droughts between 2007 and 2010 in Syria due to the changing climate have been reported as a stimulant to the Syrian unrest [83]. The droughts aggravated water crisis leading to severe agricultural and livestock losses for about 1.3 million people out of which 800,000 were affected severely [84]. It also resulted in the exodus of people from the afflicted villages to the cities [85]. With the projected decrease in annual precipitation by –30 to –85.2% for Syria [86], there may be increased aridity, losses of land productivity, increases in crop water demand and increasing frequency of droughts can increase huge economic loss and more conflicts in Syria.

## 6. Conclusions

The present study was conducted to understand the effect of recent changes in climate on aridity and the shift of arid lands in Syria between 1951–1980 and 1981–2010. Trends in precipitation, temperature and PET were evaluated under the cause of aridity shift and the impact of aridity. Finally, the aridity shift in different land uses of Syria was evaluated to understand the impacts of aridity shifts. The results revealed an expansion of arid land in Syria. The major shift of aridity was observed for semi-arid and dry-sub humid lands. About 6.21% of semi-arid land was observed to shift to arid class and 5.91% dry-sub humid land to semi-arid land between 1951–1980 and 1981–2010. The decrease in rainfall is considered as the major cause of increasing aridity in Syria. Besides, the rising temperature was observed to play a role in aridity shift in less arid regions in the northwest. The analysis of aridity shifts in respect of land use revealed that forested and agricultural lands would be the most affected by aridity shift. This may cause loss of agricultural productivity and impacts of food security of the country if mitigation actions are not initiated. The climate data used in this study are associated with some forms of uncertainty and thus the results obtained are also. In the future, different gridded data could be used to estimate uncertainty in the aridity shift in Syria. The PET can be estimated using different methods and their impacts on aridity shifts can be analyzed to evaluate the uncertainty associated with PET estimation methods on the aridity index.

**Author Contributions:** The idea was conceptualized through a group discussion in the participation of authors. M.R.H., M.S.S. and K.A. gathered the required data; S.S., M.S.N. and K.A. developed program code to analyze the data; M.R.H., M.S.S. and G.F.Z. run the code to prepare the results; E.-S.C., S.K. and M.S.N. interpreted the results. All contributed in writing the research article.

**Funding:** This research was funded by SeoulTech.

**Acknowledgments:** We are grateful to the Land Surface Hydrology Research Group of Princeton University for providing free access to the Global Meteorological Forcing Dataset for Land Surface Modeling (PGF) used in this study.

**Conflicts of Interest:** The authors declare no conflicts of interest. The funders had no role in the design of the study; in the collection, analyses, or interpretation of data; in the writing of the manuscript, or in the decision to publish the results.

## References

1. Wang, X.-J.; Elmahdi, A.; Zhang, J.-Y.; Shahid, S.; Liao, C.-H.; Zhang, X.; Liu, Y.-G. Water use and demand forecasting model for coal-fired power generation plant in China. *Environ. Dev. Sustain.* **2019**, *21*, 1675–1693. [[CrossRef](#)]
2. Pour, S.H.; Abd Wahab, A.K.; Shahid, S.; Wang, X. Spatiotemporal changes in aridity and the shift of drylands in Iran. *Atmos. Res.* **2020**, *233*. [[CrossRef](#)]
3. Nashwan, M.S.; Ismail, T.; Ahmed, K. Flood susceptibility assessment in Kelantan river basin using copula. *Int. J. Eng. Technol.* **2018**, *7*, 584–590. [[CrossRef](#)]
4. Khan, N.; Shahid, S.; Ismail, T.; Ahmed, K.; Nawaz, N. Trends in heat wave related indices in Pakistan. *Stoch. Environ. Res. Risk Assess.* **2018**, *33*, 1–16. [[CrossRef](#)]
5. Iqbal, Z.; Shahid, S.; Ahmed, K.; Ismail, T.; Nawaz, N. Spatial distribution of the trends in precipitation and precipitation extremes in the sub-Himalayan region of Pakistan. *Theor. Appl. Climatol.* **2019**. [[CrossRef](#)]
6. Nashwan, M.S.; Ismail, T.; Ahmed, K. Non-Stationary Analysis of Extreme Rainfall in Peninsular Malaysia. *J. Sustain. Sci. Manag.* **2019**, *14*, 17–34.
7. Ahmed, K.; Shahid, S.; Nawaz, N.; Khan, N. Modeling climate change impacts on precipitation in arid regions of Pakistan: A non-local model output statistics downscaling approach. *Theor. Appl. Climatol.* **2019**, *137*, 1347–1364. [[CrossRef](#)]
8. Shiru, M.S.; Shahid, S.; Shiru, S.; Chung, E.S.; Alias, N.; Ahmed, K.; Dioha, E.C.; Sa'adi, Z.; Salman, S.; Noor, M.; et al. Challenges in water resources of Lagos mega city of Nigeria in the context of climate change. *J. Water Clim. Chang.* **2019**. [[CrossRef](#)]
9. Dai, A. Drought under global warming: A review. *Wiley Interdiscip. Rev. Clim. Chang.* **2011**, *2*, 45–65. [[CrossRef](#)]

10. Qutbudin, I.; Shiru, M.S.; Sharafati, A.; Ahmed, K.; Al-Ansari, N.; Yaseen, Z.M.; Shahid, S.; Wang, X. Seasonal Drought Pattern Changes Due to Climate Variability: Case Study in Afghanistan. *Water* **2019**, *11*, 1096. [[CrossRef](#)]
11. Shiru, M.S.; Shahid, S.; Chung, E.-S.; Alias, N. Changing characteristics of meteorological droughts in Nigeria during 1901–2010. *Atmos. Res.* **2019**, *223*, 60–73. [[CrossRef](#)]
12. Alamgir, M.; Mohsenipour, M.; Homsy, R.; Wang, X.; Shahid, S.; Shiru, M.S.; Alias, N.E.; Yuzir, A. Parametric Assessment of Seasonal Drought Risk to Crop Production in Bangladesh. *Sustainability* **2019**, *11*, 1442. [[CrossRef](#)]
13. Liu, B.; Sun, J.; Liu, M.; Zeng, T.; Zhu, J. The aridity index governs the variation of vegetation characteristics in alpine grassland, Northern Tibet Plateau. *PeerJ* **2019**, *7*. [[CrossRef](#)] [[PubMed](#)]
14. Koutroulis, A.G. Dryland changes under different levels of global warming. *Sci. Total Environ.* **2019**, *655*, 482–511. [[CrossRef](#)] [[PubMed](#)]
15. Feng, S.; Fu, Q. Expansion of global drylands under a warming climate. *Atmos. Chem. Phys.* **2013**, *13*, 10081–10094. [[CrossRef](#)]
16. Parkes, S.D.; McCabe, M.F.; Griffiths, A.D.; Wang, L.; Chambers, S.; Ershadi, A.; Williams, A.G.; Strauss, J.; Element, A. Response of water vapour D-excess to land–atmosphere interactions in a semi-arid environment. *Hydrol. Earth Syst. Sci.* **2017**, *21*, 533–548. [[CrossRef](#)]
17. Ahmed, K.; Shahid, S.; Wang, X.; Nawaz, N.; Khan, N. Spatiotemporal changes in aridity of Pakistan during 1901–2016. *Hydrol. Earth Syst. Sci.* **2019**, *23*, 3081–3096. [[CrossRef](#)]
18. Salman, S.A.; Shahid, S.; Ismail, T.; Chung, E.-S.; Al-Abadi, A.M. Long-term trends in daily temperature extremes in Iraq. *Atmos. Res.* **2017**, *198*, 97–107. [[CrossRef](#)]
19. Hadi Pour, S.; Abd Wahab, A.K.; Shahid, S.; Wang, X. Spatial Pattern of the Unidirectional Trends in Thermal Bioclimatic Indicators in Iran. *Sustainability* **2019**, *11*, 2287. [[CrossRef](#)]
20. Sediqi, M.N.; Shiru, M.S.; Nashwan, M.S.; Ali, R.; Abubaker, S.; Wang, X.; Ahmed, K.; Shahid, S.; Asaduzzaman, M.; Manawi, S.M.A. Spatio-Temporal Pattern in the Changes in Availability and Sustainability of Water Resources in Afghanistan. *Sustainability* **2019**, *11*, 5836. [[CrossRef](#)]
21. IPCC. *Climate Change 2014: Impacts, Adaptation, and Vulnerability-Part B: Regional Aspects-Contribution of Working Group II to the Fifth Assessment Report of the Intergovernmental Panel on Climate Change*; Cambridge University Press: Cambridge, UK, 2014.
22. Salman, S.A.; Shahid, S.; Ismail, T.; Al-Abadi, A.M.; Wang, X.-J.; Chung, E.-S. Selection of gridded precipitation data for Iraq using compromise programming. *Measurement* **2019**, *132*, 87–98. [[CrossRef](#)]
23. Nashwan, M.S.; Shahid, S. Spatial distribution of unidirectional trends in climate and weather extremes in Nile river basin. *Theor. Appl. Climatol.* **2019**, *137*, 1181–1199. [[CrossRef](#)]
24. Araghi, A.; Martinez, C.J.; Adamowski, J.; Olesen, J.E. Spatiotemporal variations of aridity in Iran using high-resolution gridded data. *Int. J. Climatol.* **2018**, *38*, 2701–2717. [[CrossRef](#)]
25. Zolfaghari, H.; Masoompour, J.; Yeganefar, M.; Akbary, M. Studying spatial and temporal changes of aridity in Iran. *Arab. J. Geosci.* **2016**, *9*, 375. [[CrossRef](#)]
26. Tabari, H.; Hosseinzadeh Talaei, P.; Mousavi Nadoushani, S.S.; Willems, P.; Marchetto, A. A survey of temperature and precipitation based aridity indices in Iran. *Quat. Int.* **2014**, *345*, 158–166. [[CrossRef](#)]
27. Şarlak, N.; Agha, O.M.A.M. Spatial and temporal variations of aridity indices in Iraq. *Theor. Appl. Climatol.* **2018**, *133*, 89–99. [[CrossRef](#)]
28. Türkeş, M. Spatial and Temporal Variations in Precipitation and Aridity Index Series of Turkey. In *Mediterranean Climate: Variability and Trends*; Bolle, H.-J., Ed.; Springer: Berlin/Heidelberg, Germany, 2003; pp. 181–213.
29. Shaban, A.; Awad, M.; Ghandour, A.J.; Telesca, L. A 32-year aridity analysis: A tool for better understanding on water resources management in Lebanon. *Acta Geophys.* **2019**, *67*, 1179–1189. [[CrossRef](#)]
30. Telesca, L.; Shaban, A.; Awad, M. Analysis of heterogeneity of aridity index periodicity over Lebanon. *Acta Geophys.* **2019**, *67*, 167–176. [[CrossRef](#)]
31. Batanouny, K.H. Climatic Aridity in the Deserts of the Middle East. In *Plants in the Deserts of the Middle East*; Springer: Berlin/Heidelberg, Germany, 2001; pp. 11–24.
32. Pereira, L. *Climate Change Impacts on Agriculture across Africa*; Oxford University Press: Oxford, UK, 2017.

33. Mall, R.K.; Gupta, A.; Sonkar, G. 2-Effect of Climate Change on Agricultural Crops. In *Current Developments in Biotechnology and Bioengineering*; Dubey, S.K., Pandey, A., Sangwan, R.S., Eds.; Elsevier: Amsterdam, The Netherlands, 2017; pp. 23–46.
34. Daher, J. *The Political Economic Context of Syria's Reconstruction: A Prospective in Light of a Legacy of Unequal Development*; The European University Institute, Robert Schuman Centre for Advanced Studies: Badia Fiesolana, Italy, 2018.
35. Ahmed, K.; Shahid, S.; Harun, S.b.; Wang, X.-J. Characterization of seasonal droughts in Balochistan Province, Pakistan. *Stoch. Environ. Res. Risk Assess.* **2016**, *30*, 747–762. [[CrossRef](#)]
36. Sa'adi, Z.; Shiru, M.S.; Shahid, S.; Ismail, T. Selection of general circulation models for the projections of spatio-temporal changes in temperature of Borneo Island based on CMIP5. *Theor. Appl. Climatol.* **2019**. [[CrossRef](#)]
37. Pour, S.H.; Shahid, S.; Chung, E.-S.; Wang, X.-J. Model output statistics downscaling using support vector machine for the projection of spatial and temporal changes in rainfall of Bangladesh. *Atmos. Res.* **2018**, *213*, 149–162. [[CrossRef](#)]
38. Nashwan, M.S.; Shahid, S.; Chung, E.-S.; Ahmed, K.; Song, Y.H. Development of Climate-Based Index for Hydrologic Hazard Susceptibility. *Sustainability* **2018**, *10*, 2182. [[CrossRef](#)]
39. Nashwan, M.S.; Shahid, S.; Wang, X.-J. Assessment of Satellite-Based Precipitation Measurement Products over the Hot Desert Climate of Egypt. *Remote Sens.* **2019**, *11*, 555. [[CrossRef](#)]
40. Shiru, M.S.; Shahid, S.; Chung, E.-S.; Alias, N.; Scherer, L. A MCDM-based framework for selection of general circulation models and projection of spatio-temporal rainfall changes: A case study of Nigeria. *Atmos. Res.* **2019**, *225*, 1–16. [[CrossRef](#)]
41. Prăvălie, R.; Bandoc, G. Aridity Variability in the Last Five Decades in the Dobrogea Region, Romania. *Arid Land Res. Manag.* **2015**, *29*, 265–287. [[CrossRef](#)]
42. Huang, J.; Ji, M.; Xie, Y.; Wang, S.; He, Y.; Ran, J. Global semi-arid climate change over last 60 years. *Clim. Dyn.* **2016**, *46*, 1131–1150. [[CrossRef](#)]
43. Gleick, P.H. Water, Drought, Climate Change, and Conflict in Syria. *Weather Clim. Soc.* **2014**, *6*, 331–340. [[CrossRef](#)]
44. Worth, R.F. Earth is parched where Syrian farms thrived. *New York Times*. 2010. Available online: <https://www.nytimes.com/2010/10/14/world/middleeast/14syria.html> (accessed on 10 December 2019).
45. Selby, J.; Dahi, O.S.; Fröhlich, C.; Hulme, M. Climate change and the Syrian civil war revisited. *Political Geogr.* **2017**, *60*, 232–244. [[CrossRef](#)]
46. Hoerling, M.; Eischeid, J.; Perlwitz, J.; Quan, X.; Zhang, T.; Pegion, P. On the increased frequency of Mediterranean drought. *J. Clim.* **2012**, *25*, 2146–2161. [[CrossRef](#)]
47. Romanou, A.; Tselioudis, G.; Zerefos, C.; Clayson, C.; Curry, J.; Andersson, A. Evaporation–precipitation variability over the Mediterranean and the Black Seas from satellite and reanalysis estimates. *J. Clim.* **2010**, *23*, 5268–5287. [[CrossRef](#)]
48. Sheffield, J.; Goteti, G.; Wood, E.F. Development of a 50-Year High-Resolution Global Dataset of Meteorological Forcings for Land Surface Modeling. *J. Clim.* **2006**, *19*, 3088–3111. [[CrossRef](#)]
49. Bojanowski, J.S.; Vrieling, A.; Skidmore, A.K. Calibration of solar radiation models for Europe using Meteostat Second Generation and weather station data. *Agric. For. Meteorol.* **2013**, *176*, 1–9. [[CrossRef](#)]
50. Nashwan, M.S.; Shahid, S. Symmetrical uncertainty and random forest for the evaluation of gridded precipitation and temperature data. *Atmos. Res.* **2019**, *230*, 104632. [[CrossRef](#)]
51. Nashwan, M.S.; Shahid, S.; Abd Rahim, N. Unidirectional trends in annual and seasonal climate and extremes in Egypt. *Theor. Appl. Climatol.* **2019**, *136*, 457–473. [[CrossRef](#)]
52. Wu, C.; Hu, B.X.; Huang, G.; Zhang, H. Effects of climate and terrestrial storage on temporal variability of actual evapotranspiration. *J. Hydrol.* **2017**, *549*, 388–403. [[CrossRef](#)]
53. Zhu, Y.; Lin, Z.; Zhao, Y.; Li, H.; He, F.; Zhai, J.; Wang, L.; Wang, Q. Flood Simulations and Uncertainty Analysis for the Pearl River Basin Using the Coupled Land Surface and Hydrological Model System. *Water* **2017**, *9*, 391. [[CrossRef](#)]
54. Barrow, C. World atlas of desertification (*United Nations Environment Programme*). Edw. Arnold Lond. **1992**, *3*, 249.
55. Berg, A.; Sheffield, J.; Milly, P.C.D. Divergent surface and total soil moisture projections under global warming. *Geophys. Res. Lett.* **2017**, *44*, 236–244. [[CrossRef](#)]

56. Donohue, R.J.; McVicar, T.R.; Roderick, M.L. Assessing the ability of potential evaporation formulations to capture the dynamics in evaporative demand within a changing climate. *J. Hydrol.* **2010**, *386*, 186–197. [[CrossRef](#)]
57. Allen, R.G.; Pereira, L.S.; Raes, D.; Smith, M. Crop evapotranspiration-Guidelines for computing crop water requirements-FAO Irrigation and drainage paper 56. *FAO Rome* **1998**, *300*, D05109.
58. Muhammad, M.K.I.; Nashwan, M.S.; Shahid, S.; Ismail, T.B.; Song, Y.H.; Chung, E.-S. Evaluation of Empirical Reference Evapotranspiration Models Using Compromise Programming: A Case Study of Peninsular Malaysia. *Sustainability* **2019**, *11*, 4267. [[CrossRef](#)]
59. Sen, P.K. Estimates of the Regression Coefficient Based on Kendall's Tau. *J. Am. Stat. Assoc.* **1968**, *63*, 1379–1389. [[CrossRef](#)]
60. Hamed, K.H. Trend detection in hydrologic data: The Mann-Kendall trend test under the scaling hypothesis. *J. Hydrol.* **2008**, *349*, 350–363. [[CrossRef](#)]
61. Shiru, M.S.; Shahid, S.; Alias, N.; Chung, E.-S. Trend Analysis of Droughts during Crop Growing Seasons of Nigeria. *Sustainability* **2018**, *10*, 871. [[CrossRef](#)]
62. Khan, N.; Shahid, S.; Ismail, T.B.; Wang, X.J. Spatial distribution of unidirectional trends in temperature and temperature extremes in Pakistan. *Theor. Appl. Climatol.* **2018**. [[CrossRef](#)]
63. Shahid, S. Recent trends in the climate of Bangladesh. *Clim. Res.* **2010**, *42*, 185–193. [[CrossRef](#)]
64. Nashwan, M.S.; Shahid, S.; Wang, X.-J. Uncertainty in Estimated Trends Using Gridded Rainfall Data: A Case Study of Bangladesh. *Water* **2019**, *11*, 349. [[CrossRef](#)]
65. Ahammed, S.J.; Homsy, R.; Khan, N.; Shahid, S.; Shiru, M.S.; Mohsenipour, M.; Ahmed, K.; Nawaz, N.; Alias, N.E.; Yuzir, A. Assessment of changing pattern of crop water stress in Bangladesh. *Environ. Dev. Sustain.* **2019**, 1–19. [[CrossRef](#)]
66. McLeod, A.I.; Hipel, K.W. Preservation of the rescaled adjusted range: 1. A reassessment of the Hurst Phenomenon. *Water Resour. Res.* **1978**, *14*, 491–508. [[CrossRef](#)]
67. Feng, H.; Zhang, M. Global land moisture trends: Drier in dry and wetter in wet over land. *Sci. Rep.* **2015**, *5*. [[CrossRef](#)]
68. Lickley, M.; Solomon, S. Drivers, timing and some impacts of global aridity change. *Environ. Res. Lett.* **2018**, *13*, 104010. [[CrossRef](#)]
69. Shifteh Some'e, B.; Ezani, A.; Tabari, H. Spatiotemporal trends of aridity index in arid and semi-arid regions of Iran. *Theor. Appl. Climatol.* **2013**, *111*, 149–160. [[CrossRef](#)]
70. Deniz, A.; Toros, H.; Incecik, S. Spatial variations of climate indices in Turkey. *Int. J. Climatol.* **2011**, *31*, 394–403. [[CrossRef](#)]
71. El Kenawy, A.M.; Lopez-Moreno, J.I.; McCabe, M.F.; Robaa, S.M.; Domínguez-Castro, F.; Peña-Gallardo, M.; Trigo, R.M.; Hereher, M.E.; Al-Awadhi, T.; Vicente-Serrano, S.M. Daily temperature extremes over Egypt: Spatial patterns, temporal trends, and driving forces. *Atmos. Res.* **2019**, *226*, 219–239. [[CrossRef](#)]
72. Shahid, S.; Harun, S.B.; Katimon, A. Changes in diurnal temperature range in Bangladesh during the time period 1961–2008. *Atmos. Res.* **2012**, *118*, 260–270. [[CrossRef](#)]
73. Nashwan, M.S.; Shahid, S.; Chung, E.-S. Development of high-resolution daily gridded temperature datasets for the central north region of Egypt. *Sci. Data* **2019**, *6*, 138. [[CrossRef](#)]
74. Gado, T.A.; El-Hagrsy, R.M.; Rashwan, I.M.H. Spatial and temporal rainfall changes in Egypt. *Environ. Sci. Pollut. Res.* **2019**, *26*, 28228–28242. [[CrossRef](#)]
75. Salman, S.A.; Shahid, S.; Ismail, T.; Rahman, N.B.A.; Wang, X.; Chung, E.S. Unidirectional trends in daily rainfall extremes of Iraq. *Theor. Appl. Climatol.* **2017**, 1–13. [[CrossRef](#)]
76. Khan, N.; Pour, S.H.; Shahid, S.; Ismail, T.; Ahmed, K.; Chung, E.-S.; Nawaz, N.; Wang, X. Spatial distribution of secular trends in rainfall indices of Peninsular Malaysia in the presence of long-term persistence. *Meteorol. Appl.* **2019**, *26*, 655–670. [[CrossRef](#)]
77. Alizadeh-Choobari, O.; Najafi, M.S. Extreme weather events in Iran under a changing climate. *Clim. Dyn.* **2018**, *50*, 249–260. [[CrossRef](#)]
78. Moreno-Jiménez, E.; Plaza, C.; Saiz, H.; Manzano, R.; Flagmeier, M.; Maestre, F.T. Aridity and reduced soil micronutrient availability in global drylands. *Nat. Sustain.* **2019**, *2*, 371–377. [[CrossRef](#)] [[PubMed](#)]
79. Chowdhury, S.; Al-Zahrani, M.; Abbas, A. Implications of climate change on crop water requirements in arid region: An example of Al-Jouf, Saudi Arabia. *J. King Saud Univ.-Eng. Sci.* **2016**, *28*, 21–31. [[CrossRef](#)]

80. Ragab, R.; Prudhomme, C. Sw-Soil and Water: Climate change and water resources management in arid and semi-arid regions: Prospective and challenges for the 21st century. *Biosyst. Eng.* **2002**, *81*, 3–34. [[CrossRef](#)]
81. Azad, N.; Behmanesh, J.; Rezaverdinejad, V.; Tayfeh Rezaie, H. Climate change impacts modeling on winter wheat yield under full and deficit irrigation in Myandoab-Iran. *Arch. Agron. Soil Sci.* **2018**, *64*, 731–746. [[CrossRef](#)]
82. Onder, D.; Akiscan, Y.; Onder, S.; Mert, M. Effect of different irrigation water level on cotton yield and yield components. *Afr. J. Biotechnol.* **2009**, *8*, 1536–1544.
83. Kelley, C.P.; Mohtadi, S.; Cane, M.A.; Seager, R.; Kushnir, Y. Climate change in the Fertile Crescent and implications of the recent Syrian drought. *Proc. Natl. Acad. Sci. USA* **2015**, *112*, 3241. [[CrossRef](#)]
84. Gökalp, D. Syria: The Making and Unmaking of a Refugee State. By Dawn Chatty. *J. Refug. Stud.* **2019**, *32*, 164–166. [[CrossRef](#)]
85. Solh, M. Tackling the Drought in Syria. Available online: <https://www.natureasia.com/en/nmiddleeast/article/10.1038/nmiddleeast.2010.206> (accessed on 9 May 2019).
86. Homsy, R.; Shiru, M.S.; Shahid, S.; Ismail, T.; Harun, S.; Al-Ansari, N.; Chau, K.-W.; Yaseen, Z.M. Precipitation projection using a CMIP5 GCM ensemble model: A regional investigation of Syria. *Eng. Appl. Comput. Fluid Mech.* **2020**, *14*, 90–106. [[CrossRef](#)]



© 2019 by the authors. Licensee MDPI, Basel, Switzerland. This article is an open access article distributed under the terms and conditions of the Creative Commons Attribution (CC BY) license (<http://creativecommons.org/licenses/by/4.0/>).